International Journal of Bifurcation and Chaos, Vol. 5, No. 6 (1995) 1487–1501
© World Scientific Publishing Company

SPIRALS IN SCALAR REACTION–DIFFUSION EQUATIONS

MICHAEL DELLNITZ
Inst für Angewandte Mathematik, Universität Hamburg, D-20146 Hamburg, Germany

MARTIN GOLUBITSKY
Dept of Mathematics, University of Houston, Houston, TX 77204-3476, USA

ANDREAS HOHMANN
Konrad-Zuse-Zentrum für Informationstechnik Berlin, D-10711 Berlin, Germany

IAN STEWART
Mathematics Institute University of Warwick, Coventry, CV4 7AL, UK

Received February 25, 1995; Revised March 30, 1995

Spiral patterns have been observed experimentally, numerically, and theoretically in a variety of systems. It is often believed that these spiral wave patterns can occur only in systems of reaction–diffusion equations. We show, both theoretically (using Hopf bifurcation techniques) and numerically (using both direct simulation and continuation of rotating waves) that spiral wave patterns can appear in a single reaction–diffusion equation [in $u(x, t)$] on a disk, if one assumes "spiral" boundary conditions ($u_r = mu_\theta$). Spiral boundary conditions are motivated by assuming that a solution is infinitesimally an Archimedian spiral near the boundary. It follows from a bifurcation analysis that for this form of spirals there are no singularities in the spiral pattern (technically there is no spiral tip) and that at bifurcation there is a steep gradient between the "red" and "blue" arms of the spiral.

1. Introduction

The Belousov–Zhabotinskii reaction is a widely studied instance of pattern formation in a reacting chemical system: see for example Tyson [1976], Vasiliev *et al.* [1987], Winfree [1990], and Zhabotinskii [1974]. It has been the subject of numerous experiments, computer simulations, and analytic investigations. The models employed range from reaction–diffusion equations to cellular automata; for recent references, see Barkley [1991a, 1991b, 1993, 1994], Barkley & Kevrekidis [1994]. Moreover, a wide range of *ad hoc* approximations have been introduced in an effort to capture different aspects of the dynamics. The observed phenomena include circular waves ("target patterns") and, most strikingly, rotating spirals. The spirals appear to be approximately Archimedean in form, that is, their "width" — the gap between successive coils — is asymptotically constant as the radius increases. In three dimensions more exotic wave forms arise, including "scroll rings"; see Winfree [1974a]. Moreover, very similar wave phenomena occur in

excitable media; see Winfree [1990] for a survey and an extensive list of references. The diversity of both the observed phenomena and the theoretical viewpoints adopted has created a large, heterogeneous, and sometimes controversial, literature. In order to focus upon mathematical issues we postpone detailed discussion to Sec. 7, at which point it also becomes possible to relate our work to the existing literature.

Although many aspects of the Belousov–Zhabotinskii reaction are now well understood, the basic mathematical mechanisms of pattern formation in reaction–diffusion equations (and others of similar kind) remain somewhat mysterious. In particular, even though spirals are commonly observed in experiments and simulations, their existence in model equations has been proved only infrequently. DeDimone *et al.* [1973] used what amounts to Hopf bifurcation to prove the existence of spiral waves in a particular reaction–diffusion equation in the plane, for which the chemical kinetics has two degrees of freedom. The radial dependence of linearized eigenfunctions involves Bessel functions $J_m(r)$ and $Y_m(r)$, and the $Y_m(r)$ term becomes infinite for $r = 0$ and thus creates a singularity at the origin. Kopell & Howard [1973] proved the existence of plane wave solutions to reaction–diffusion equations. Tyson ([1976], p. 99) emphasized the rotating wave structure of spirals and suggested looking for an asymptotic representation. Greenberg [1976] used asymptotic methods to establish the existence of spiral waves in some cases. Auchmuty [1984] proves the existence of rotating waves resulting from Hopf bifurcation in *systems* of reaction–diffusion equations (that is, with at least two degrees of freedom for the local chemical kinetics) posed on a two-dimensional circular disk with Neumann boundary conditions.

The aim of this paper is to use the techniques of equivariant bifurcation theory — whose emphasis on symmetry is especially well adapted to questions of pattern formation — to prove a rigorous bifurcation theorem for spiral waves in a planar domain. For simplicity we work within the framework of scalar reaction–diffusion equations, but it will become obvious that the ideas are valid more generally. The relation between these waves and the patterns observed in the Belousov–Zhabotinskii reaction itself is not entirely clear, and further work is needed to resolve a number of key issues — again, see Sec. 7. However, our results do establish a number of interesting theoretical points, among them the following:

- Spiral waves can be created by Hopf bifurcation in rotationally symmetric systems of reaction–diffusion equations.
- Spiral waves can occur in *scalar* reaction–diffusion equations.
  This is perhaps surprising, because the occurrence of oscillatory kinetics in the local chemical reaction requires local state variables with at least two degrees of freedom.
- The solutions obtained in this paper do *not* possess a singularity at the tip (or center) of the spiral. On the contrary, the variable corresponding to chemical concentration varies smoothly throughout the domain. The same is true of the linearized eigenfunctions at the Hopf bifurcation point.

We qualify these remarks by adding that the spiral waves obtained by using our approach are unstable — but "only just". They have precisely one positive Floquet exponent, which may be very close to zero. In consequence, they persist over long periods of time in direct simulations of the PDEs. It is reasonable to presume that the spiral waves that we produce by Hopf bifurcation can be asymptotically stable in *system* of reaction diffusion equations.

We also note at the outset that we are employing Hopf bifurcation as a technique for proving the existence of solutions in a parametrized family of equations. We are not asserting that in the corresponding physical systems the usual experimental scenarios necessarily involve Hopf bifurcation. In fact, as can be seen in Kness *et al.* [1992], Barkley [1994], and Barkley & Kevrekidis [1994], numerical models of typical experimental scenarios reveal the presence of an "infinite period" bifurcation in which the spiral "comes in from infinity", becoming more tightly wound and with shorter period. There is no direct correspondence between the way we explore parameter space to prove the existence of spirals, and the way an experiment would explore parameter space.

By thinking about the problem within the recently developed framework of equivariant bifurcation theory, much of the previous work can be understood and motivated in a straightforward fashion, as follows. Spiral waves are time-periodic states — so it is reasonable to suppose that spirals might arise by Hopf bifurcation. Spirals are *rotating waves*; that is, their time evolution is identical to spatial rotation. Thus, spirals are most likely to

arise in models having rotational symmetry, so it makes sense to pose the PDEs on a circular disk. The motivation for using Neumann boundary conditions has a different source: it comes from the chemical experiments. These are often done in circular dishes, so that no-flux boundary conditions seem appropriate.

Any reaction–diffusion model satisfying the above conditions is symmetric under the orthogonal group O(2) in the plane. The general theory of symmetry-breaking Hopf bifurcations in systems with O(2) symmetry is well known; see, for example, Golubitsky *et al.* [1988], Chap. XVII. In this case, the purely imaginary eigenvalues associated with the Hopf bifurcation are double. There are two types of time-periodic solution — rotating waves and standing waves. Further, in these systems there is a (nonlinear) competition between these two states.

An important point, however, is that the linearized operators obtained from reaction–diffusion equations with Neumann boundary conditions are self-adjoint. Thus, single equations must have real eigenvalues, and Hopf bifurcation is not possible. However, systems of reaction–diffusion equations with O(2) symmetry can have purely imaginary eigenvalues and can undergo Hopf bifurcation. Indeed Auchmuty [1984] showed that for certain parameter ranges in the Brusselator model, a trivial solution first loses stability via a Hopf bifurcation (of the double eigenvalue variety), leading to a rotating wave. Moreover, Auchmuty noted that a spiral pattern can be seen in the level contours of the solutions. The critical eigenfunctions are related to Bessel functions, and spirals occur as contours.

In this paper, we take a somewhat different, although related, approach. We try to find the spiral pattern by choosing "spiral" boundary conditions. We arrive at these slightly nonstandard boundary conditions as follows. Suppose that we look for Archimedean spirals. The assumption of equal spiral widths implies that far from the center of the spiral the function u that determines the spiral profile is *approximately* of the form

$$u(r, \theta) = v(mr + \theta)\,.$$

Here, (r, θ) are polar coordinates and m is constant. Suppose for the sake of motivation that near the boundary the solution u has *exactly* this form. Then infinitesimally we find the *spiral boundary condition*

$$u_r = m u_\theta \quad \text{on } \partial B_R\,, \tag{1.1}$$

where B_R is a ball of radius R. Since $mr+(\theta+2\pi) = m(r + \frac{2\pi}{m}) + \theta$, the number $\frac{2\pi}{m}$ is the asymptotic wavelength of the spiral and may be interpreted as the *spiral width.*

Remark 1.1. It is not necessary to interpret the circle ∂B_R as the *boundary* of the domain. The "spiral boundary condition" can also be thought of as a constraint imposed on some circle inside the domain, which forces a spiral structure — at least near that circle. We discuss this point further in Sec. 7.

This approach is analogous to finding spatially periodic solutions to reaction–diffusion systems by assuming periodic boundary conditions. Spiral boundary conditions (1.1) are SO(2)-symmetric rather than O(2)-symmetric. Rotating waves (but not standing waves) are to be expected in symmetry-breaking Hopf bifurcations in systems with SO(2) symmetry; see Golubitsky *et al.* [1988], p. 359.

We will adopt this approach to prove the existence of spiral waves via Hopf bifurcation. For simplicity, consider a single scalar reaction–diffusion equation

$$u_t = \Delta u + \lambda u + f(u) \quad \text{in } B_R\,, \tag{1.2}$$

satisfying spiral boundary conditions (1.1). Here, f is a real-valued function with $f(0) = 0$ and λ is a real parameter. We will show that there are time-periodic solutions to (1.2) with contour lines having the shape of spirals.

The reason that we are able to find points of Hopf bifurcation in this setting is that the corresponding linearized operator is no longer self-adjoint, so that purely imaginary eigenvalues are possible. Indeed, we will show that an infinite number of Hopf bifurcations from the trivial solution occur in (1.2). All of these solutions are rotating waves with spiral contours.

Since there is a steady state bifurcation in (1.2) for $\lambda = 0$, all of these Hopf bifurcations lead — at least locally — to unstable rotating waves. However, we have carried out numerical simulations which show that spiral waves persist for a very long integration time. We explain this phenomenon by computing the Floquet multipliers along the branch of spirals. The results show that for increasing values of λ there are "almost stable" spirals, in the sense that just one Floquet multiplier is larger than 1 in absolute value, but only just larger.

The behavior at the center of the spiral has attracted specific attention in the past. In fact, it is

often suggested that a spiral wave exhibits a singularity at its center and, moreover, that the type of this singularity is related to the spiraling behavior. We examine this suggestion in Sec. 7. The viewpoint of this paper is quite different: the spirals studied here are considered to be as a result of global constraints on the system (namely, spiral "boundary" conditions). As already remarked, our solutions — like those of several other authors listed in Sec. 7 — have no singularity at the center of the spiral (or elsewhere). Indeed, with the cubic nonlinearity chosen in Sec. 6 below, the solution is identically zero at the origin, and smooth throughout the entire plane. Thus we consider the boundary conditions to be more crucial than a hypothetical central singularity.

A more detailed outline of the paper is as follows. In Sec. 2 we investigate the scaling and symmetry properties of (1.2). We show that we can either set $m = 1$ and consider the radius R as a parameter, or we can set $R = 1$ and consider the constant m as a parameter. In Sec. 3 we use separation of variables to derive a nonlinear equation involving complex Bessel functions, whose solutions correspond to parameter values for Hopf bifurcations from the trivial solution. Using an idea from Renardy [1982] (see also Golubitsky *et al.* [1988]), we show in Sec. 4 how the computation of Floquet exponents for the rotating waves is simplified by the SO(2) symmetry of the problem. Next we show by numerical computation that the solutions emanating from the Hopf bifurcation points are spiral in form, and that in numerical integrations they persist for a long time.

2. Scaling and Symmetry Properties

Consider the boundary value problem

$$\begin{aligned} u_t = u_{rr} + \frac{1}{r}u_r + \frac{1}{r^2}u_{\theta\theta} + \lambda u + f(u) \quad &\text{in } B_R\,, \\ u_r = m u_\theta \quad &\text{on } \partial B_R\,, \end{aligned} \tag{2.1}$$

where m is nonzero and R is positive. This is a reaction–diffusion equation in polar coordinate form. If $u(t, r, \theta)$ is a solution of (2.1) then $u(t, r, \theta + \varphi)$ is a solution for each $\varphi \in [0, 2\pi)$, so the equation has SO(2) symmetry.

Remark 2.1. Let u_n and u_s denote the normal and tangential derivatives of u. Then we can rewrite (2.1) in the simple form

$$\begin{aligned} u_t &= \Delta u + \lambda u + f(u) \quad &\text{in } B_R\,, \\ u_n &= mRu_s \quad &\text{on } \partial B_R\,. \end{aligned}$$

We begin by investigating the scaling properties of (2.1). To do so we rescale the variables by introducing:

$$\tau = \beta t\,, \quad \rho = \varepsilon r\,, \quad \varphi = \kappa\theta\,,$$

where β and ε are positive real numbers, and $\kappa = \pm 1$; and we define a new function

$$v = Au\,,$$

where A is a nonzero real number.

Substituting these rescaled variables into (2.1) leads to the equivalent boundary value problem

$$\begin{aligned} v_\tau = \frac{\varepsilon^2}{\beta}\left(v_{\rho\rho} + \frac{1}{\rho}v_\rho + \frac{1}{\rho^2}v_{\varphi\varphi}\right) + \frac{\lambda}{\beta}v + \frac{A}{\beta}f\left(\frac{1}{A}v\right) \quad &\text{in } B_{\varepsilon R}\,, \\ \varepsilon v_\rho = m\kappa v_\varphi \quad &\text{on } \partial B_{\varepsilon R}\,. \end{aligned}$$

After setting

$$\varepsilon^2 = \beta \quad \text{and} \quad \tilde{\lambda} = \lambda/\beta\,,$$

we are left with two possibilities:

(i) We set $\varepsilon = m\kappa$ which leads to the simplified problem

$$\begin{aligned} v_\tau = v_{\rho\rho} + \frac{1}{\rho}v_\rho + \frac{1}{\rho^2}v_{\varphi\varphi} + \tilde{\lambda}v + \frac{A}{m^2}f\left(\frac{1}{A}v\right) \quad &\text{in } B_{\tilde{R}}, \\ v_\rho = v_\varphi \quad &\text{on } \partial B_{\tilde{R}}\,, \end{aligned} \tag{2.2}$$

where $\tilde{R} = |m|R$.

(ii) We set $\varepsilon = 1/R$ and obtain

$$\begin{aligned} v_\tau = v_{\rho\rho} + \frac{1}{\rho}v_\rho + \frac{1}{\rho^2}v_{\varphi\varphi} + \tilde{\lambda}v + AR^2 f\left(\frac{1}{A}v\right) \quad &\text{in } B_1\,, \\ v_\rho = \tilde{m}v_\varphi \quad &\text{on } \partial B_1\,, \end{aligned} \tag{2.3}$$

where $\tilde{m} = |m|R > 0$.

Note that κ is chosen so that $\tilde{R} > 0$ or $\tilde{m} > 0$.

The above scaling arguments show that, as expected, we may either set the spiral width equal to unity and consider a radius (R) of appropriate size, or we may set the radius of the disk to unity and consider a spiral width ($2\pi/m$) of appropriate size.

3. The Linearized Problem

For simplicity of notation, we henceforth omit the tildes from $\tilde{\lambda}$ and $\tilde{m}$ in (2.2, 2.3). We also replace φ by θ. In this section, we show that the system (2.2) possesses Hopf bifurcation points for positive values of λ. By SO(2)-equivariance these bifurcations imply the existence of nontrivial rotating waves, see Golubitsky *et al.* [1988], p. 359. Hence, we want to find this type of solution for suitable parameter values in the linear boundary value problem.

The trivial solution $u = 0$ of (2.2) undergoes a steady-state bifurcation at $\lambda = 0$, with a constant eigenfunction. This can be checked by linearizing (2.2) at $u = 0$ as follows:

$$\begin{aligned} u_t &= u_{rr} + \frac{1}{r}u_r + \frac{1}{r^2}u_{\theta\theta} + \lambda u \quad \text{in } B_R, \\ u_r &= m u_\theta \qquad\qquad\qquad \text{on } \partial B_R. \end{aligned} \tag{3.1}$$

We solve (3.1) by separation of variables, assuming that u takes the form

$$u(r, \theta, t) = e^{i\omega t} e^{in\theta} u_n(r). \tag{3.2}$$

Substituting (3.2) into the PDE (3.1) leads to the ODE

$$i\omega u_n(r) = u_n''(r) + \frac{1}{r}u_n'(r) - \frac{n^2}{r^2}u_n(r) + \lambda u_n(r).$$

Writing $\mu = \lambda - i\omega$, this becomes

$$\frac{1}{\mu}u_n''(r) + \frac{1}{\mu r}u_n'(r) + \left(1 - \frac{n^2}{\mu r^2}\right)u_n(r) = 0.$$

Introducing the complex variable $z = \sqrt{\mu}r$, we arrive at the complex version of Bessel's equation (see Whittaker & Watson [1948] or Sneddon [1957]):

$$v_n''(z) + \frac{1}{z}v_n'(z) + \left(1 - \frac{n^2}{z^2}\right)v_n(z) = 0. \tag{3.3}$$

Assuming that $v_n(0)$ is defined — that is, that there is no singularity at the origin — solutions of (3.3) are complex Bessel functions $J_n(z)$, so u_n has the form

$$u_n(r) = J_n(\sqrt{\mu}r).$$

[Without this regularity assumption solutions may also involve the Bessel function $Y_n(z)$.] Finally, we must take the boundary condition into account. This leads to the equation

$$\sqrt{\mu}J_n'(\sqrt{\mu}R) = inmJ_n(\sqrt{\mu}R), \tag{3.4}$$

and using the identity

$$J_n'(z) = J_{n-1}(z) - \frac{n}{z}J_n(z),$$

we obtain

$$\sqrt{\mu}J_{n-1}(\sqrt{\mu}R) - n\left(\frac{1}{R} + im\right)J_n(\sqrt{\mu}R) = 0.$$

According to (2.2) and (2.3) we now have two possible ways to simplify this equation. We consider either

$$\sqrt{\mu}J_{n-1}(\sqrt{\mu}R) - n\left(\frac{1}{R} + i\right)J_n(\sqrt{\mu}R) = 0 \tag{3.5}$$

or

$$\sqrt{\mu}J_{n-1}(\sqrt{\mu}) - n(1 + im)J_n(\sqrt{\mu}) = 0. \tag{3.6}$$

For $\omega \neq 0$, we expect each complex solution $\lambda - i\omega$ of this equation to correspond to a Hopf bifurcation to rotating waves of period $2\pi/\omega$ in the original nonlinear problem for the parameter value λ. Of course, it is necessary to check the usual nondegeneracy conditions, such as the eigenvalue crossing condition, but these will be valid generically. Note that for $n = 0$ the Eq. (3.4) becomes

$$J_0'(\sqrt{\mu}R) = -J_1(\sqrt{\mu}R) = 0,$$

which has only real solutions. These correspond to steady-state bifurcations leading to target-like patterns. In fact, the first steady-state bifurcation occurs for $\lambda = 0$ where spatially constant solutions bifurcate, and the second such bifurcation is encountered at $\sqrt{\lambda}R = 3.83$, right after the first Hopf bifurcation (see Sec. 6). We will see that for $n > 0$ the eigenfunctions correspond to n armed spirals.

Remark 3.1. Equation (3.1) defines a Fredholm operator of index $2 - 2m$ (see Hörmander [1976]). In particular, we get index 0 for $m = 1$. Therefore, a Liapunov–Schmidt reduction along the lines of Golubitsky & Schaeffer [1985], Chap. VIII, is possible, and Hopf bifurcation points are well defined.

For the computation of the solutions of the complex nonlinear Eq. (3.5), we use Newton's method combined with a pathfollowing method, where either the radius R or n is the parameter. (Of course, only solutions where n is an integer are relevant.) To obtain suitable initial guesses we have computed the eigenvalues of the discretized linear operator (see Sec. 5.1) for a fixed radius R.

Figure 1 shows how the behavior of a branch of solutions of (3.5) varies with R for $n = 1$. In particular, both λ and ω tend to zero as R tends to infinity. There is numerical evidence that this behavior occurs for all values of n. In Fig. 2, we show the dependence of the solution branch on n. Here we can see that λ is a monotonically increasing function of n. Finally, in Figs. 3–5, we show contour plots of eigenfunctions for $n = 0, 1, 2$. Note that when $n = 0$ we find a target-like pattern; for $n = 1$ we find a standard one-armed spiral; and for $n = 2$ we find a two-armed spiral.

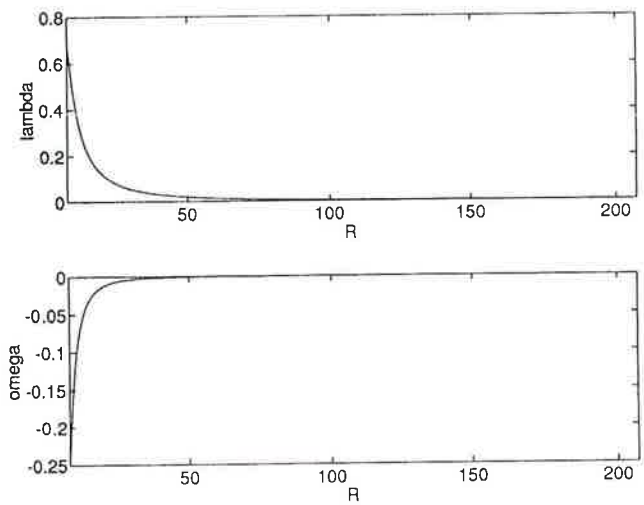

Fig. 1. Dependence of a solution of (3.5) on the radius R when $n = 1$.

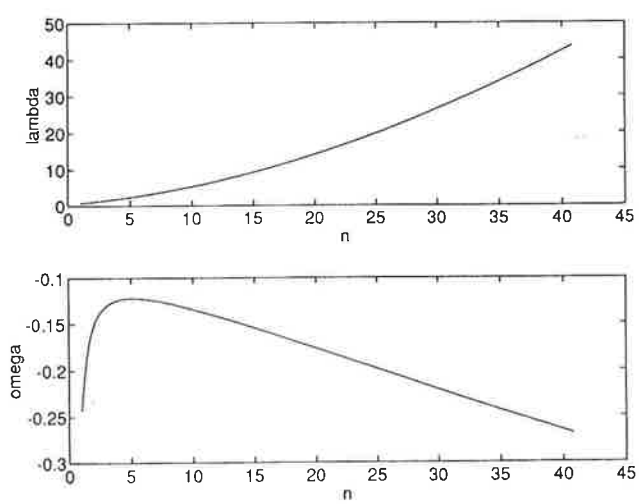

Fig. 2. Dependence of a solution of (3.5) on the magnitude of n when $R = 8$.

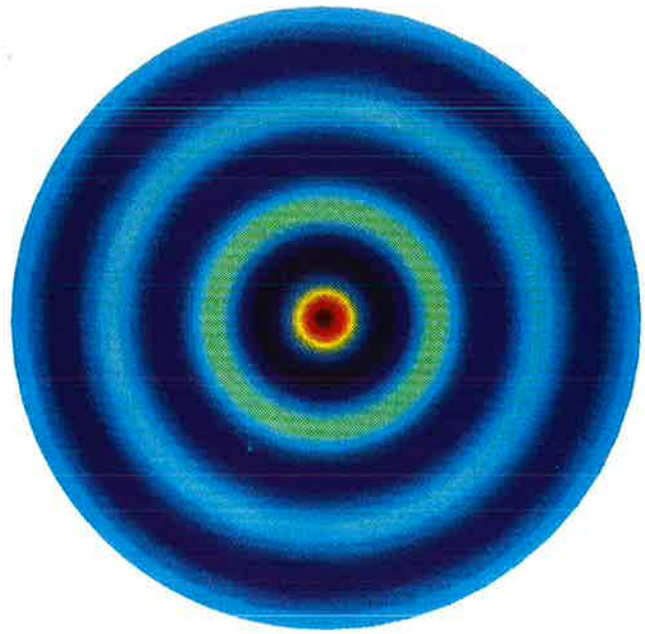

Fig. 3. Eigenfunction for $n = 0$, $\lambda = 0.6680$, and $R = 24$.

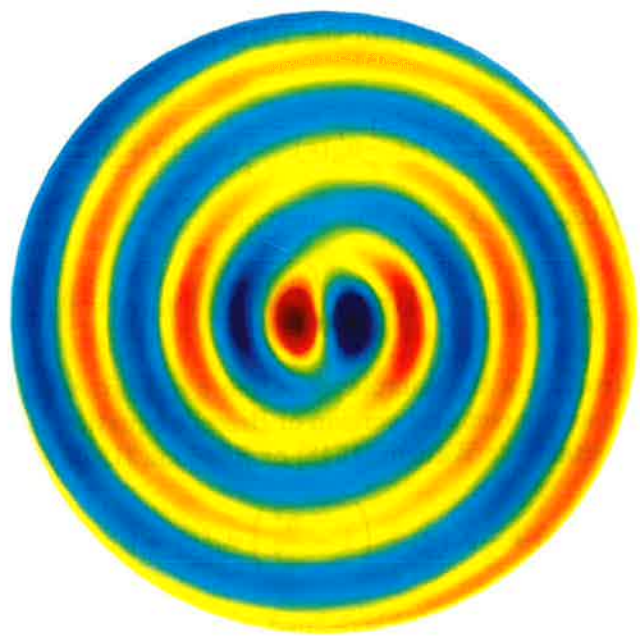

Fig. 4. Eigenfunction for $n = 1$, $\lambda = 0.6598$, $R = 24$, and frequency $\omega = 0.0767$.

4. Floquet Theory

We now consider the stability of the spiral solution (within the space of rotating waves — we do not consider more general perturbations). By SO(2)-symmetry, the periodic solutions emanating from

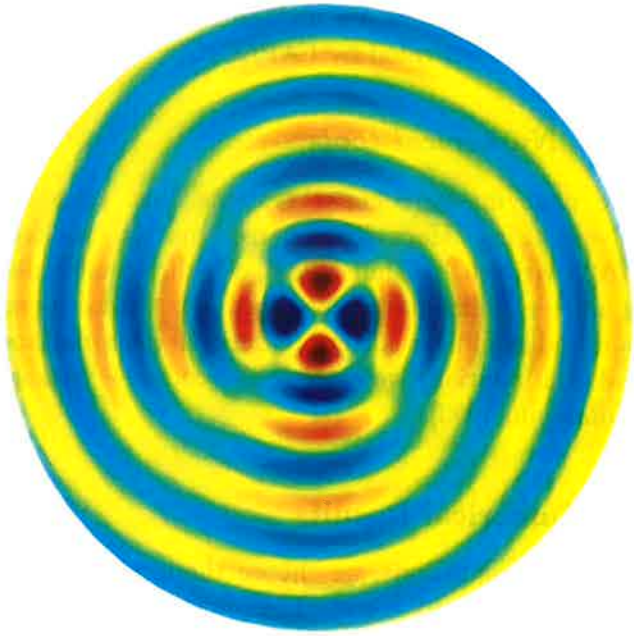

Fig. 5. Eigenfunction for $n = 2$, $\lambda = 1.3036$, $R = 24$, and frequency $\omega = 0.0617$.

the Hopf bifurcation points are rotating waves, that is, they are solutions of the form

$$u(r, \theta, t) = v(r, \theta + \omega t)$$

for some function $v(r, \theta)$. Substituting the time derivative

$$\left.\frac{\partial u}{\partial t}\right|_{t=0} = \omega v_\theta(r, \theta)$$

of u at $t = 0$ into the differential Eq. (2.1), we see that the wave form v satisfies the parameter-dependent nonlinear equation

$$\begin{aligned} v_{rr} + \tfrac{1}{r} v_r + \tfrac{1}{r^2} v_{\theta\theta} - \omega v_\theta + \lambda v + f(v) = 0 \quad & \text{in } B_R\,, \\ v_r = m v_\theta \quad & \text{on } \partial B_R\,. \end{aligned} \tag{4.1}$$

In the computation of the corresponding Floquet exponents we again make use of the SO(2)-equivariance of the evolution equation $u_t = F(u)$ and the fact that the spiral is a rotating wave. It is known that, in this case, the computations can be simplified and we adapt the proof of Proposition 6.4 in Chap. XVI, Golubitsky *et al.* [1988]. To avoid inconsistencies in notation we denote an element of SO(2) that is usually written in the form $\phi \in [0, 2\pi)$ by γ_ϕ.

The variational equation is given by

$$z_t(r, \theta, t) - DF(u(r, \theta, t))z(r, \theta, t) = 0\,.$$

Writing $z(r, \theta, t) = \tilde{z}(r, \theta + \omega t, t)$ we obtain

$$\begin{aligned} 0 &= z_t(r, \theta, t) - DF(u(r, \theta, t))z(r, \theta, t) \\ &= \omega \tilde{z}_\theta(r, \theta + \omega t, t) + \tilde{z}_t(r, \theta + \omega t, t) \\ &\quad - DF(v(r, \theta + \omega t))\tilde{z}(r, \theta + \omega t, t) \\ &= \gamma_{\omega t}[\omega \tilde{z}_\theta(r, \theta, t) + \tilde{z}_t(r, \theta, t) \\ &\quad - DF(v(r, \theta))\tilde{z}(r, \theta, t)]\,. \end{aligned}$$

Hence, $z_t(r, \theta, t) - DF(u(r, \theta, t))z(r, \theta, t) = 0$ if and only if

$$\tilde{z}_t(r, \theta, t) = DF(v(r, \theta))\tilde{z}(r, \theta, t) - \omega \tilde{z}_\theta(r, \theta, t)\,.$$

But this implies that

$$\tilde{z}(r, \theta, t) = \exp\left[t\left(DF(v(r, \theta)) - \omega \frac{\partial}{\partial \theta}\right)\right]\tilde{z}(r, \theta, 0)$$

and using $z(r, \theta, 2\pi/\omega) = \tilde{z}(r, \theta, 2\pi/\omega)$ and $z(r, \theta, 0) = \tilde{z}(r, \theta, 0)$ we obtain

$$\begin{aligned} &z(r, \theta, 2\pi/\omega) \\ &\quad = \exp\left[2\pi\left(\frac{1}{\omega} DF(v(r, \theta)) - \frac{\partial}{\partial \theta}\right)\right] z(r, \theta, 0)\,. \end{aligned}$$

Thus, to obtain an estimate of the magnitude of Floquet exponents we must compute the eigenvalues of the operator

$$\frac{1}{\omega} DF(v(r, \theta)) - \frac{\partial}{\partial \theta}\,. \tag{4.2}$$

5. Numerical Computation of Spirals

In this section, we employ numerical computations to find parameter values at which the branches of periodic solutions bifurcate supercritically from the Hopf bifurcation points given by solutions of (3.5). Since the trivial steady-state solution has already lost its stability at $\lambda = 0$, the bifurcating rotating waves are locally unstable. However, our numerical computations show that there is just one unstable eigenvalue. Moreover, this eigenvalue tends to zero from above for increasing values of λ.

For the direct simulation of the time-dependent system, we use the method of lines, combining a finite difference scheme in space with an adaptive extrapolation integrator in time.

5.1. *Discretization by finite differences in space*

For the spatial discretization of the partial differential operator we employ finite differences in polar coordinates, using the formulation (2.2). We have chosen a tensor product mesh defined by equidistant partitions of the intervals $[0, R]$ and $[0, 2\pi]$. The derivatives with respect to r and θ are approximated by central differences, except for the radial derivative u_r at the boundary, where we use one-sided differences.

Applying these schemes to the boundary condition, we can express the values at the boundary as a linear function of the values at the grid points inside the disk. With this we obtain a discretization of the operator including the (discretized) boundary conditions.

5.2. *Discretization in time*

Using the methods of lines, we first discretize in space as described in the previous subsection, and then use a standard integrator to solve the resulting system of ODEs. Here, we employ the integration code EULSIM, based on the linearly implicit Euler discretization, combined with extrapolation and adaptive order and step-size control [Deuflhard, 1989].

5.3. *Continuation of rotating waves*

For the computation of the rotating wave solutions, we use a predictor–corrector method for the parameter-dependent nonlinear Eq. (4.1). Because of the $\mathbf{SO}(2)$ symmetry this problem is underdetermined, with ω as implicit parameter. Hence, we use a Gauss–Newton method as the corrector and combine it with a tangential predictor. This approach is in the spirit of the methods proposed by Deuflhard [1984] for computing periodic solutions. The dominant eigenvalues of the rotating waves are computed by a similar continuation process, using a linear predictor and the inverse power method as a corrector. In this way, we exploit the sparse structure of the linear (but nonsymmetric) system. Thus, the computation of the dominant eigenvalues requires less work than that of the rotating wave solution. To verify the eigenvalue computations and to obtain appropriate initial values for the continuation process, we use the full matrix eigenvalue solvers provided by LAPACK.

5.4. *Numerical tools*

The nonsymmetric linear systems that arise are solved using Harwell's sparse matrix package MA28 written by Duff [1980], which is embedded in a C++ sparse matrix package. For time integration and nonlinear solvers (Gauss–Newton method and continuation) we employ the code++ package [Hohmann, 1993].

6. Numerical Results

In our computations, we choose the nonlinearity f in (2.2) to be $f(v) = \alpha v^3$. The parameter α may be scaled to ± 1 by suitable choice of A in (2.2). We mainly consider the parameter values

$$R = 8 \quad \text{and} \quad \alpha = -1\,.$$

With this choice, the first Hopf bifurcation occurs at $\lambda = 0.2200$. In all the computations we choose 30 discretization points in the radial direction and 50 in the angular direction.

Figure 6 shows the branch of rotating wave solutions that emanates from $u = 0$ when $\lambda = 0.2200$. The corresponding radial factor of the eigenfunction is related to the real or imaginary part of the complex Bessel function J_1 [see (3.5)].

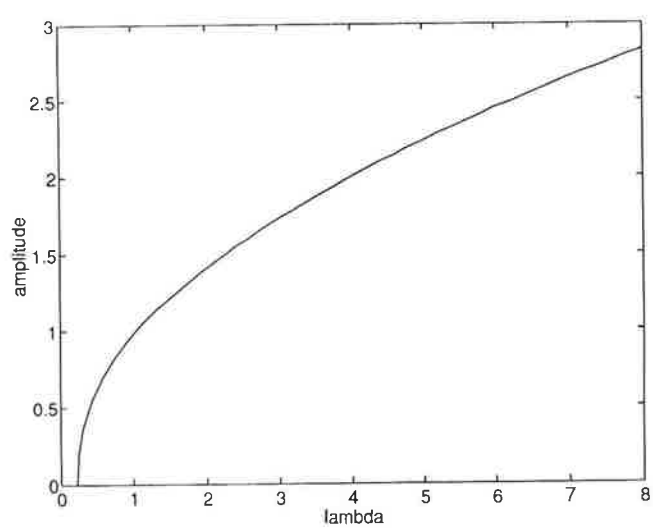

Fig. 6. The branch of rotating wave solutions that emanates when $\lambda = 0.2200$.

Next, we compute the Floquet exponents by calculating the eigenvalues of (4.2). Because of SO(2) symmetry, there is one zero eigenvalue along this branch. As noted in the Introduction, there is also one positive eigenvalue. The three eigenvalues along this branch with largest real part are shown in Fig. 7. The positive eigenvalue approaches zero, while all other eigenvalues remain nonpositive. In consequence, the spirals appear to be stable in direct simulations for a very long integration time,

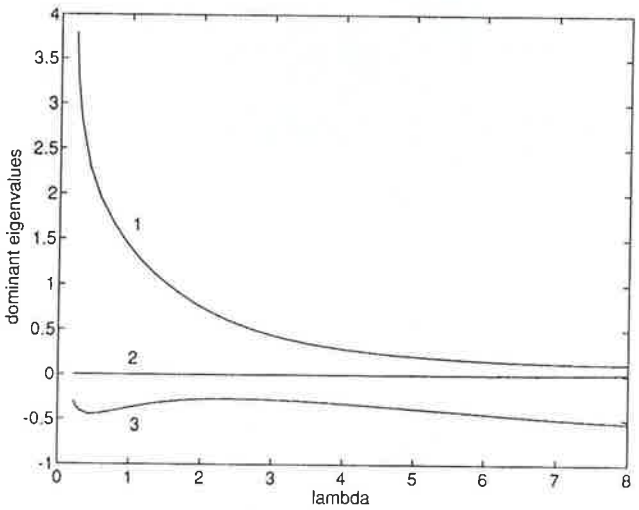

Fig. 7. Dominant three eigenvalues along a branch of rotating waves.

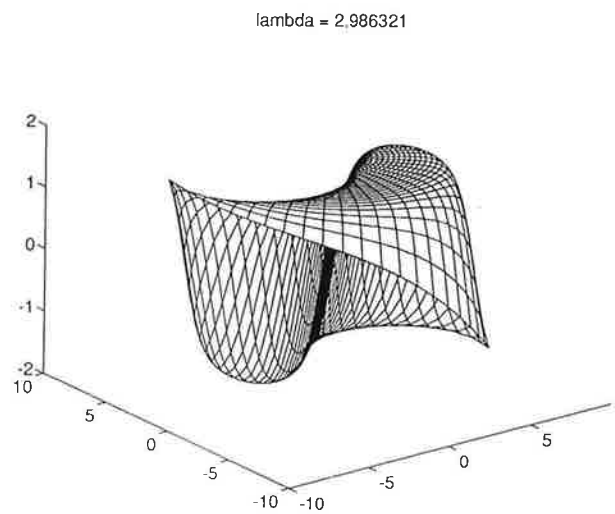

Fig. 9. Rotating wave for $\lambda = 2.986321$, $R = 8$, and frequency $\omega = 0.111$.

lambda = 2.986320

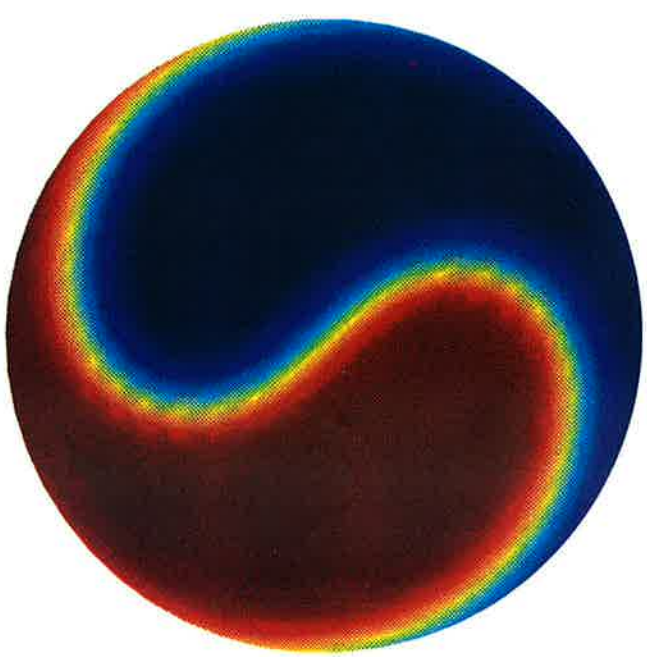

Fig. 8. Rotating wave for $\lambda = 2.986321$, $R = 8$, and frequency $\omega = 0.111$.

lambda = 7.999867

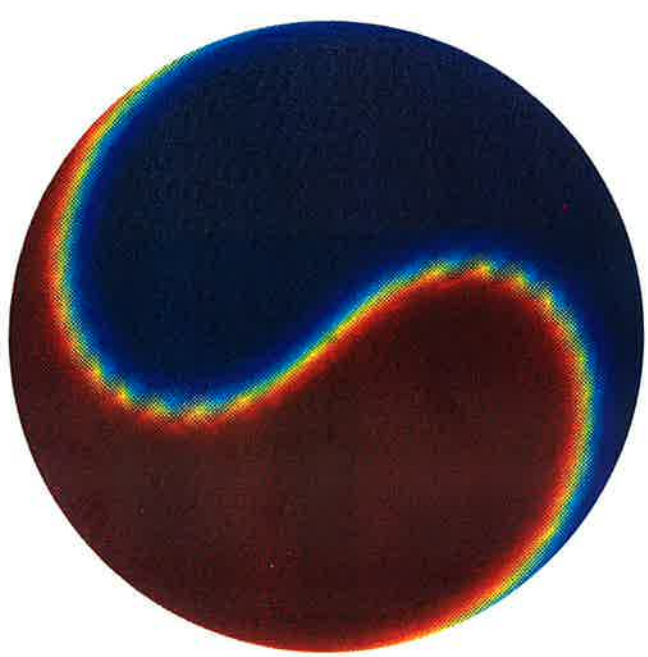

Fig. 10. Rotating wave for $\lambda = 7.999867$. $R = 8$, and frequency $\omega = 0.102$.

until the (weak) instability eventually takes over. Moreover, this phenomenon becomes more pronounced as λ becomes larger.

Figures 8 and 10 show contour plots of two spirals lying on this branch of rotating waves. At each instant of time these spirals have a nontrivial symmetry: a rotation by 180 degrees combined with the order two symmetry $u \to -u$. This additional symmetry is present because we have chosen the nonlinearity to be an odd function (here, purely cubic). Because of this, the symmetry of the problem becomes $\mathbf{SO}(2) \times \mathbb{Z}_2$ rather than just $\mathbf{SO}(2)$. The width of the computed spirals pictured in Figs. 8–10 appears to be in good agreement with the theoretical spiral width, which is $2\pi/8 \approx 0.8$. The computations show that the layer between the two parts of the spiral becomes extremely steep with increasing values of λ. We illustrate this phenomenon in Figs. 9 and 11.

Because of this steep gradient the numerical computations are more difficult for larger values of λ and for larger spatial domains. In fact, in order to obtain reliable numerical results for these values of λ it would be necessary to increase the number of discretization points substantially, preferably combining this with some adaptive mesh selection. For these reasons, we have not increased the size of the domain beyond $R = 8$ in most of our computations. However, Fig. 12 shows a rotating wave solution computed for $R = 12$ by direct simulation. As for $R = 8$, this solution appears to be unstable. Again, we find good agreement with the theoretical spiral width of $2\pi/12 \approx 0.5$.

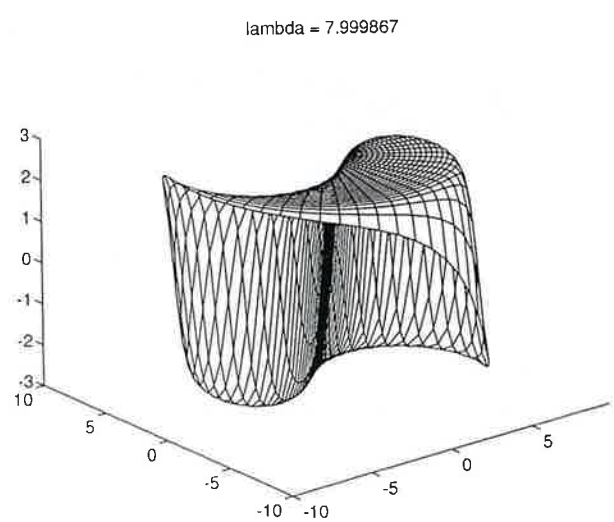

Fig. 11. Rotating wave for $\lambda = 7.999867$, $R = 8$, and frequency $\omega = 0.102$.

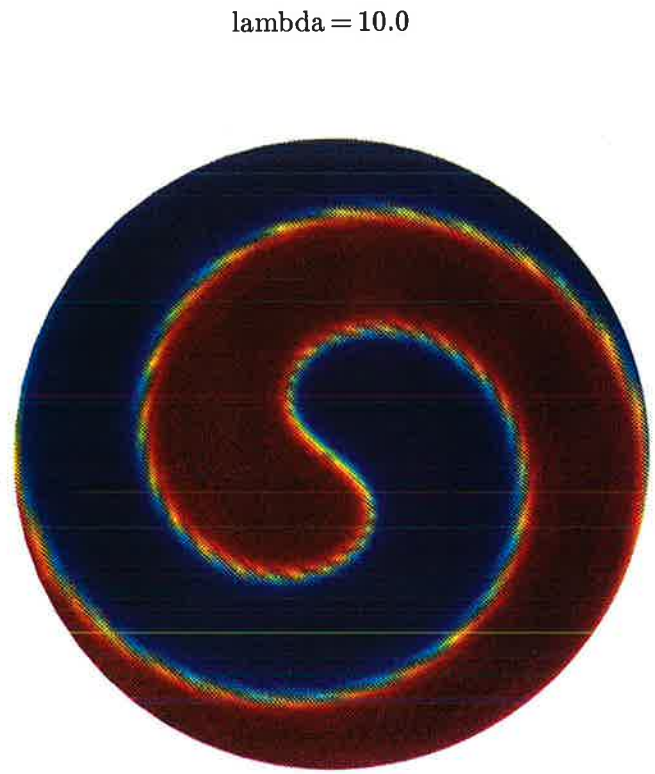

Fig. 12. A spiral for $\lambda = 10.00$.

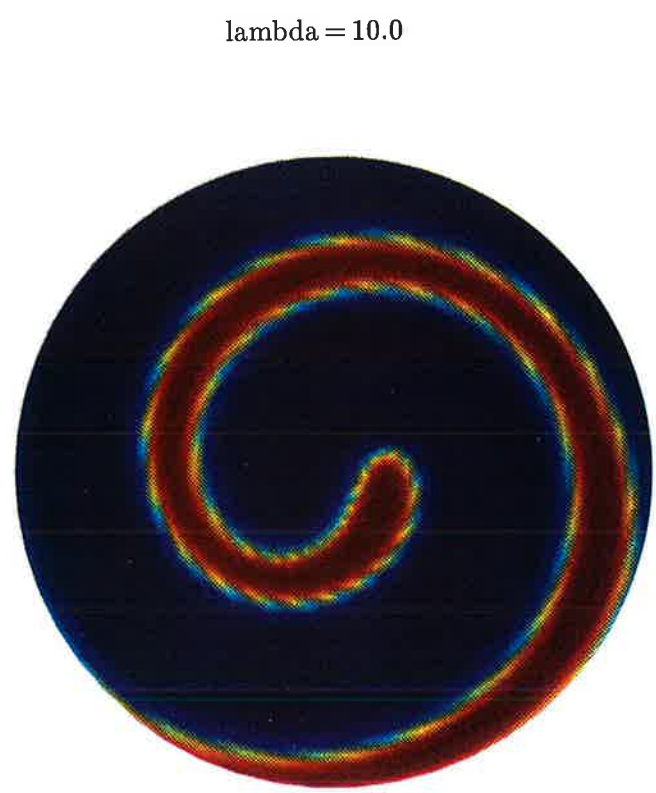

Fig. 13. A spiral for $\lambda = 10.00$, where a quadratic term has been added.

Finally, in order to explore the effect of breaking the extra $\mathbb{Z}_2$ symmetry introduced by the cubic nonlinearity, we show one computation where a quadratic term has been added to the equation. See Fig. 13. Note that the spiral is no longer equally spaced and that the red/blue transition is different from the blue/red transition.

7. Relation to Previous Work

In this section, we relate our work to existing results and hypotheses. Our discussion focuses on various more or less relevant issues, but makes no pretension to completeness.

We begin with a brief history of the Belousov–Zhabotinskii reaction and its associated patterns. Oscillating chemical reactions seem to have first been reported by William Bray in 1921, in the decomposition of hydrogen peroxide into water and oxygen in the presence of an iodine catalyst. Unfortunately, his results were widely disbelieved because they were thought — wrongly — to contradict the second law of thermodynamics. In consequence, the topic stagnated until 1958, when B. P. Belousov observed periodic oscillations in a mixture of citric and sulfuric acid, potassium bromate, and a cerium salt. In 1963, A. M. Zhabotinskii modified Belousov's recipe, replacing cerium salts with iron salts, so that changes in ionic concentrations could be visualized as a dramatic red/blue color change. The recipe has been modified several times since, to improve the ease of repetition of the experiment and the robustness of the result: recipes may be found in Winfree [1990], p. 301, and Cohen & Stewart [1994], p. 461. The central feature of modern versions of the reaction is the presence of bromate ions in an acid solution, which oxidize some organic substrate.

In one common form of the experiment, the chemicals are mixed in appropriate quantities, and in a particular order, and stirred together in a dish. The mixture is blue at first but rapidly turns red: the color is homogeneous across the entire dish. If it is left for a period of about 10–20 minutes, however, blue spots form spontaneously. The spots grow, and their centers turn red. Soon the dish contains several independent "target patterns" of concentric red and blue rings. These patterns merge in a characteristic manner when they meet.

The formation of target patterns is an example of spontaneous symmetry-breaking. The spatially homogeneous state is unstable, and when it loses stability through small random inhomogeneities the result is a state with circular symmetry about some point. The translational symmetries (of an infinite planar model) are broken. It is customary to hypothesize some physical pointlike "seed" that causes the symmetry to break in an experimental setting — such as a bubble, an impurity, or a scratch on the glass dish. Such "seeds" may perhaps relate to singularities in the solution, but symmetry-breaking may occur for reasons other than a pointlike singularity. Since it is *target patterns*, not spirals, that form *spontaneously*, it is not clear that a pointlike singularity would be an appropriate physical seed for spirals. In order to create spirals experimentally, it is necessary to either tilt the dish slightly and then restore it to the horizontal, or to insert a hot wire (which is usually moved across the wave to create some kind of curve singularity). The effect is to produce a topological dislocation in the wave pattern, and spiral forms result. They appear to be stable, but this is not absolutely clear because experiments usually continue for less than an hour. After that period of time the reagents are used up: the solution is actually a dynamical transient on the way to a different — and uninteresting — equilibrium. However, it is normal to model the system as if the reagents are constantly and uniformly replenished — as indeed they are in some experiments — and there are no good reasons to expect instability of the spiral wave in such circumstances.

As noted earlier, the spirals seen in experiments are approximately Archimedean in form — that is, their width is roughly constant. The precise shape of the spiral has been a topic of considerable research. In early work, the "spiral" metaphor was perhaps taken too literally, a tendency that was exposed when Guckenheimer [1976] (and independently S. Hastings and J. M. Greenberg in unpublished work, see Winfree [1990], p. 309–310) proved that concentration contours in a reaction–diffusion equation cannot all be congruent concentric spirals. (From the symmetry viewpoint such a structure is, in any case, extremely unlikely, requiring a connection between rotations in the domain and changes in the value of a chemical concentration; moreover, it is far stronger than is required to explain the observations.)

In 1946, Wiener & Rosenblüth [1946] had introduced the idea of an "involute" wave form — a spiral shaped like the involute of a circle — when approximating the shape of excitation waves on the surface of a living heart. This idea was developed by Stibitz & Rytand [1968] in relation to

experiments on animal hearts, and by Durston [1973] to patterns in slime mould. Some authors have modelled Belousov–Zhabotinskii spirals using involutes. Winfree [1990], p. 245, onwards, exposed the rather unreasonable assumptions involved in the involute model. It is clear that both Archimedean and involute spirals are just convenient geometrical approximations; and it is arguable that a more accurate description relates to the Bessel functions that occur in both our linearized eigenfunctions and those obtained earlier by DeDimone *et al.* [1973]. For large radii the width of the spiral becomes asymptotically constant in all these geometric models. This is reasonable if we make the entirely plausible assumption that there is a natural wavelength for traveling plane waves and that the spiral waves are asymptotically planar — that is, their curvature becomes negligible. This assumption is used, for example, in the work of Kopell & Howard [1973].

Winfree [1990] pioneered a point of view on targets, spirals, and related patterns, which emphasized the phase of the local chemical oscillation at each point in the medium. The underlying model is that at each spatial location the system is oscillating around the *same* limit cycle in the local chemical kinetics, and that diffusion acts as a small short-range coupling which creates some kind of global phase coherence. For example, the phase is constant along the distinctive and sharp wavefront where a blue region is invading a red one. This model leads to topological restrictions on the pattern of phases, and hence on the contours of appropriate chemical concentrations; it also leads to the influential idea that there must be a "phase singularity" at or near the tip of the spiral — a point at which the phase becomes ill-defined.

However, Winfree also noted that this phase model involves approximations that are not always appropriate. In particular, the state of the reaction near the center of the spiral varies smoothly, despite the phase singularity. This was shown for non-oscillating excitable kinetics by Gul'ko & Petrov [1972], Karfunkel [1975], and Winfree [1974b]; and for nonexcitable oscillating kinetics by Erneux & Herschkowitz-Kauffman [1977], Yamada & Kuramoto [1976], and Cohen *et al.* [1978].

Winfree [1990], pp. 248–249, explains this phenomenon in terms of the dimensionality of the local kinetics, in effect observing that the apparent topological restrictions imposed by the occurrence of a phase singularity do not conflict with smoothness for a *system* of reaction–diffusion equations in which the chemical kinetics involves two or more variables. We concur with his discussion, but would go one step further, because, as our figures show, we also observe smoothly varying concentrations in a *scalar* system. The reason, we believe, lies not in the dimensionality of the local kinetics, but in the modelling assumptions involved in the phase approximation. Phase is not a uniquely defined concept; it is only *relative* phase that has an invariant meaning. The relative phase of two *identical* wave forms is a precise concept; but the phase of a single wave form, or the relative phase of two different wave forms, involve a more or less arbitrary choice. The phase of an arbitrary wave form can of course be fixed by assuming that the maximum value of the wave form occurs at zero phase. This provides a unique phase — at least it does so generically, on the assumption that the wave form does not have two equal maxima within a single period. However, with this definition the phase need not vary continuously with the wave form (imagine an M-shaped wave whose maximum occurs at the left-hand peak, and slowly deform the heights of the two peaks so that the left-hand one moves down until the right-hand one becomes the global maximum). Once phase ceases to be a continuous function of wave form, topological restrictions lose much of their force. It appears possible to analyze the movements of maxima using singularity theory: this would presumably provide a rigorous foundation for Winfree's approach when the wave form remains approximately constant, but it would lead to different topological restrictions when it does not.

To be more precise: at each point x of the domain of the PDE, consider the solution $u(x, t)$ with fixed x. Winfree's phase model assumes that for all x the function $u(x, t)$ is identical up to a phase shift; that is, that $u(x, t) = u(y, t + \phi(x, y))$ for all points x, y in the domain (except those for which there is a phase singularity). Experiments (both chemical and numerical) show this to be approximately true unless x or y are near the origin. Thus the phase model is good for providing global restrictions on the geometry of waves far from the origin, but breaks down near the origin. As is observed on page 248 of Winfree [1990], "The 'pivot' is an idealization ... which serves a purpose only when not examined too closely."

Kness *et al.* [1992] studied a one-dimensional model of an excitable medium and derived an O(2)-symmetric normal form, thereby introducing explicit symmetry considerations. This approach

was extended in Barkley [1993, 1994] and Barkley & Kevrekidis [1994]: the emphasis is on the Euclidean group symmetry of the entire plane. This approach has led to a considerably increased understanding of the dynamics of spirals, including "meandering" of the tip, and the infinite-period bifurcation associated with the onset of spirals in numerical models related to particular experimental scenarios, discussed in the introduction.

Having described the context provided by previous work, we now discuss how the results of this paper fit into it. On the positive side, we have established several results which, apart from numerical calculations which in principle could be avoided by making suitable estimates, are rigorously proved. As noted in the introduction, they include the following:

- Spiral waves can be created by Hopf bifurcation in rotationally symmetric systems of reaction–diffusion equations.
- Spiral waves can occur in *scalar* reaction–diffusion equations.
- Spiral solutions need not possess a singularity at the tip of the spiral (or anywhere else).

We repeat that we are not claiming that Hopf bifurcation is the appropriate mechanism for reproducing the behavior found in particular experiments or numerical models. We are using Hopf bifurcation as a technique for proving the existence of solutions at suitable points in a mathematical parameter space.

The spirals observed experimentally exhibit a very sharp transition where blue regions of the domain are expanding into the red — see, for example, Fig. 5 on p. 313 of Winfree [1990], Tyson [1976], p. 62, finds similarly sharp transitions in the "oregonator" model of the chemical kinetics of the Belousov–Zhabotinskii reaction, introduced originally by Field & Noyes [1972]. The oscillations that he finds are "hard excitations", that is, they correspond to a limit cycle that coexists with a stable equilibrium state — unlike the limit cycle that appears near the bifurcation point in Hopf bifurcation. We must distinguish between the sharp wave front in the Belousov–Zhabotinskii reaction (indicating a limit cycle of large amplitude) and a hard excitation (which coexists with a stable rest state and is therefore necessarily of large amplitude). Our numerical results show that in these nonlinear reaction–diffusion equations a supercritical Hopf bifurcation can lead to a wave front that steepens progressively, and rapidly, past the bifurcation point. It is therefore not necessary to have the "hard excitation" scenario in order to produce a sharp wave front. Indeed, it is not even necessary to have a subcritical Hopf bifurcation which subsequently "turns round" and becomes stable — a common way to produce a large-amplitude limit cycle via Hopf bifurcation.

The wave front that arises in our model possesses one awkward feature, however: the transition is equally sharp when the red region propagates into the blue. This is a consequence of the additional $\mathbb{Z}_2$ symmetry noted in Sec. 6, which is created by the cubic nonlinearity. As seen in Fig. 13, an asymmetric nonlinearity — for example, one with a further quartic term, or maybe a quadratic one — produces an asymmetric wave form. It seems plausible that a suitable choice of nonlinearity could reproduce the sharp blue/red transition while providing a gradual red/blue transition.

Our results also show that it is *not* necessary for the local chemical kinetics to possess a limit cycle in order for the reaction–diffusion equation to produce this apparent hard excitation. (This calls the "hard excitation" terminology into question since there is no suitable phase space in which it applies.) Our equation has a one-dimensional state space for the kinetics, which cannot support a limit cycle. Even though our solutions are (marginally) unstable, they establish this point clearly. The source of the oscillatory behavior seems to be the ODE (3.3), which is *second* order; this fact traces back ultimately to the second order partial derivatives on the *spatial diffusion* terms in the PDE (2.1). This raises the question to what extent features of the wave form have traditionally been attributed to the local "reaction" dynamics, when in fact they are due to diffusive coupling of the local dynamics across some finite region. Perhaps it would be worth reexamining the usual assumptions, bearing this in mind.

Next, we make some remarks about the role of the "spiral" boundary conditions. Figures 6 and 7 show "yin–yang" shaped patterns which do not resemble those found in experiments, for two reasons, both of which have been discussed previously. The first reason is that our model equation has an extra symmetry. The second reason is the assumption that the boundary of the disk B_R corresponds to the boundary of a dish in which the reaction takes place. To put it another way, the width of the spiral is too large compared to the size of dish.

As remarked already, this feature of our pictures is largely an artifact of the parameter values chosen for our numerical simulations, and would presumably disappear if we were to solve the equations for larger values of R. (As noted previously, this simulation will require substantially greater numerical effort.) Figure 10 goes some way towards establishing this point.

However, there is another possible interpretation altogether which offers some advantages and should certainly be borne in mind. Spiral boundary conditions are a mathematical device for proving the occurrence of spiral patterns; they do not correspond in any natural way to physical behavior near the boundary of an actual container. They can be viewed as a theoretical ansatz whose role is to select, from the infinitely varied range of possible solutions, a small subset with the desired spiral form. Spiral boundary conditions therefore represent a constraint that the solution is required to satisfy on some chosen circle; but there is no obligation to interpret this circle as the boundary of the container. For example, the container might be a larger circular dish [to retain SO(2) symmetry] and the circle ∂B_R might be an arbitrary reference circle some distance inside the container but concentric with it.

The approach adopted in this paper might perhaps extend to more exotic wave forms. For example, a similar kind of ansatz, imposing suitable "infinitesimal" conditions on a solution over the surface of a torus in three-dimensional space, might perhaps lead to a similarly rigorous proof of the existence of scroll waves.

Finally, we note that the general viewpoint introduced in this paper is not restricted to reaction–diffusion equations, nor is it limited to scalar PDEs. We have worked under these restrictions in order to keep the calculations as simple as possible, but in principle there should be no difficulty in relaxing them. The crucial feature of the model that leads to spiral waves is the SO(2) symmetry.

Acknowledgments

We thank Giles Auchmuty, Dwight Barkley, Folkmar Bornemann, Norman Dancer, John Guckenheimer, Barbara Keyfitz, Bill Langford, and Hans Othmer for helpful conversations. This research was supported in part by NSF Grant DMS-9403624 (MG), ONR Grant N00014-94-1-0317 (MG, MD), the Texas Advanced Research Program (003652037) (MG), the Deutsche Forschungsgemeinschaft and the Konrad-Zuse-Zentrum für Informationstechnik Berlin (MD, AH), NSF U.S.–Australia Cooperative Research Grant (INT-9114207), a grant from EPSRC (INS), and a Laboratory Twinning grant from the EU (INS). The idea of spiral boundary conditions first began to emerge during a visit of MG and INS to the Fields Institute, and was made explicit when MG subsequently visited Warwick University. MD and AH acknowledge the hospitality of the Department of Mathematics of the University of Houston, where most of this work was carried out.

References

Auchmuty, J. F. G. [1984] "Bifurcation analysis of reaction–diffusion equations V: rotating waves on a disc," in *Partial Differential Equations and Dynamical Systems*, ed. Fitzgibbon, W. E., Res. Notes Math. **101** (Pitman, Marshfield, MA), p. 173–181.

Barkley, D. [1991] "A model for fast computer simulation of waves in excitable media," *Physica* **D49**, 61–70.

Barkley, D. "Linear stability analysis of rotating spiral waves in excitable media," preprint, Princeton 1991.

Barkley, D. "Euclidean symmetry and the dynamics of rotating spiral waves," preprint, U Texas, Austin 1993.

Barkley, D. [1994] "Spiral meandering," in *Chemical Waves and Patterns*, eds. Kapral, R. & Showalter, K. (Kluwer, Amsterdam), p. 163–188.

Barkley, D. & Kevrekidis, I. [1994] "A dynamical systems approach to spiral wave dynamics, *Chaos* **4**, 453–460.

Barkley, D., Kness, M. & Tuckerman, L. S. [1990] "Spiral-wave dynamics in a simple model of excitable media: the transition from simple to compound rotation," *Phys. Rev.* **A42**, 2489–2492.

Cohen, D. S., Neu, J. C. & Rosales, R. R. [1978] "Rotating spiral wave solutions of reaction-diffusion equations," *SIAM J. Appl. Math.* **35**, 536–547.

Cohen, J. & Stewart, I. N. [1994] *The Collapse of Chaos* (Viking, New York).

DeSimone, J. A., Beil, D. L. & Scriven, L. E. [1973] "Ferroin-collodion membranes: dynamic concentration patterns in planar membranes," *Science* **180**, 946–948.

Deuflhard, P. [1984] "Computation of periodic solutions of nonlinear ODEs," *BIT* **24**, 456–466.

Deuflhard, P. [1989] "Uniqueness theorems for stiff ODE initial value problems," in *Proceedings 13th Biennial Conference on Numerical Analysis* (University of Dundee).

Duff, I. S., Erisman, A. M. & Reid, J. K. [1986] *Direct Methods for Sparse Matrices* (Oxford University Press, Oxford).

Durston, A. J. [1973] "*Dictyostelium discoideum* aggregation fields as excitable media," *J. Theor. Biol.* **42**, 483–504.

Erneux, T. & Herschkowitz-Kauffman, M. [1977] "Rotating waves as asymptotic solutions of a model chemical reaction," *J. Chem. Phys.* **66**, 248–250.

Field, R. J. & Noyes, R. M. [1972] "Explanation of spatial band propagation in the Belousov reaction, *Nature* **237**, 390–392.

Golubitsky, M. & Schaeffer, D. G. [1985] "*Singularities and Groups in Bifurcation Theory*, Vol. I, *Applied Math. Sci.* **51** (Springer-Verlag, New York).

Golubitsky, M., Stewart, I. & Schaeffer, D. G. [1988] *Singularities and Groups in Bifurcation Theory*, Vol. II, *Applied Math. Sci.* **69**, (Springer-Verlag, New York).

Greenberg, J. M. [1976] "Periodic solutions to reaction–diffusion equations," *SIAM J. Appl. Math.* **30**, 199–205.

Guckenheimer, J. [1976] "Constant velocity waves in oscillating chemical reactions," in *Structural Stability, the Theory of Catastrophes, and Applications in the Sciences*, ed. Hilton, P., *Lecture Notes in Math.* **525**, 99–103.

Gul'ko, F. B. & Petrov, A. A. [1972] "Mechanism of formation of closed pathways of conduction in excitable media," *Biofizika* **17**, 261–270.

Hohmann, A. [1993] "An implementation of extrapolation codes in C++," Technical Report TR 93-8, Konrad-Zuse-Zentrum Berlin.

Hörmander, L. [1976] *Linear Partial Differential Operators* (Springer-Verlag, New York).

Karfunkel, H. R. [1975] *Zur Theorie der Anregbarkeit und Ausbreitung von Erregungswellen in Chemischen Reaktionssystemen*, Dissertation, Univ. Tübingen.

Kness, M., Tuckerman, L. S. & Barkley, D. [1992] "Symmetry-breaking bifurcations in one-dimensional excitable media," *Phys. Rev.* **A46**, 5054–5062.

Kopell, N. & Howard, L. N. [1973] "Plane wave solutions to reaction–diffusion equations," *Studies Appl. Math.* **52**, 291–328.

Renardy, M. [1982] "Bifurcation from rotating waves," *Arch. Rational Mech. Anal.* **75**, 49–84.

Sneddon, I. N. [1957] *Elements of Partial Differential Equations* (McGraw-Hill, New York).

Stibitz, G. R. & Rytand, D. A. [1968] "On the path of the excitation wave in atrial flutter," *Circulation* **37**, 75–81.

Tyson, J. J. [1976] *The Belousov-Zhabotinskii Reaction*, Lecture Notes in Biomath. **10** (Springer-Verlag, Berlin).

Vasiliev, V. A., Romanovskii, Yu. M., Chernavskii, D. S. & Yakhno, V. G. [1987] *Autowave Processes in Kinetic Systems, Mathematics and Its Applications* (Soviet Series) (Reidel, Dordrecht).

Whittaker, E. T. & Watson, G. N. [1948] *A Course of Modern Analysis* (Cambridge University Press, Macmillan, New York).

Wiener, N. and Rosenblüth, A. [1946] "The mathematical formulation of the problem of conduction of impulses in a network of connected excitable elements, specifically in cardiac muscle," *Arch. Inst. Cardiologia de Mexico* **16**, 205–265.

Winfree, A. T. [1974] "Two kinds of wave in an oscillating chemical solution," *Farad. Symp. Chem. Soc.* **9**, 38–46.

Winfree, A. T. [1974] "Rotating chemical reactions," *Scientific American* **230**(6), 82–95.

Winfree, A. T. [1990] *The Geometry of Biological Time*, 2nd ed. (Springer-Verlag, Berlin).

Yamada, T. & Kuramoto, Y. [1976] "Spiral waves in a nonlinear dissipative system," *Prog. Theor. Phys.* **55**, 2035–2036.

Zhabotinskii, A. M. [1974] *Spontaneously Oscillating Concentrations* (in Russian) (Science Publishers, Moscow).